Original article

Prediction of skin permeation by chemical compounds using the artificial membrane, Strat-M™

Takashi Uchida, Wesam R. Kadhum, Sayumi Kanai, Hiroaki Todo, Takeshi Oshizaka, Kenji Sugibayashi*

Faculty of Pharmaceutical Sciences, Josai University, 1-1 Keyakidai, Sakado, Saitama 350-0295, Japan.

To whom correspondence should be addressed:

Kenji Sugibayashi, Ph.D.

Faculty of Pharmaceutical Sciences, Josai University,

Keyakidai, Sakado, Saitama 350-0295, Japan.

Tel.: 049-271-7367

Fax: 049-271-8137

E-mail: sugib@josai.ac.jp

1. Introduction

In the past 20 years, more than 35 transdermal delivery systems (TDDSs) have been approved in the US, EU, and Japan(Murthy, 2012). *In vitro* skin permeation experiments are considered to be useful in the development of new TDDSs. Artificial membranes using a parallel artificial membrane permeability assay, PAMPA (Akamatsu et al., 2009; Avdeef et al., 2007), and skin-PVPA model (Palac et al., 2014) are currently used to select orally administered drug candidates in a short experimental period. However, the selection of compound candidates from a large chemical library is time-consuming because the skin permeation rates of chemical compounds are known to be markedly lower than those through other mucosal membranes. Therefore, synthesized artificial membranes (Hatanaka et al., 1990; Sugibayashi et al., 2010) and three-dimensional cultured human skin models (Kano et al., 2010; Poumay et al., 2004) have been used as alternatives to human and animal skins in the development of TDDSs. Previous studies examined the *flux* or permeability coefficients, *P*, of chemical compounds through alternative membranes and those through excised human or animal skin (Kano et al., 2010; Morimoto et al., 1992; Scott et al., 1986). Sinkó *et al.*, recently described (SinkÃ et al., 2012) PAMPA incorporated with human ceramide analogues and fatty acids in the stratum corneum. Although PAMPA could roughly predict human skin permeability, a 1:1 correlation was not obtained between the *P* values of chemicals through the synthetic membrane and human skin. This finding suggested that this membrane may not be sufficiently sensitive to reflect the physicochemical properties of penetrants.

The physicochemical properties of drugs, such as their molecular weights and the lipophilic/hydrophilic balance (i.e., octanol/ buffer apparent distribution ratio at a

particular pH, log $K_{o/w}$), have been shown to markedly affect permeability through skin (Potts and Guy, 1992; Lian et al., 2008; Riviere and Brooks, 2011). Most drugs utilized in TDDSs have a molecular weight under 500 Daltons (Bos and Meinardi, 2000), and the P value through skin was previously reported to markedly decrease with an increase in molecular weight over 500 Daltons. Furthermore, elevations were observed in the P values of drugs with an increase in the log $K_{o/w}$. Thus, the P value can be further divided into two parameters; diffusion (DL^{-2}) and partition (KL) parameters (Okamoto et al., 1988), where D, K and L are the diffusion coefficient, partition coefficient, and thickness of the membrane, respectively. These parameters can be easily obtained from *in vitro* skin permeation experiments, the values of which depend on the characteristics as well as penetrant properties of the membrane. Therefore, the acquisition of these parameters for alternative membranes may prove very useful in understanding membrane characteristics and their similarities (or difference) to human and animal skins.

An *in silico* approach has also been attempted in order to predict the P values of chemical compounds through skin with their physicochemical properties (Potts and Guy, 1992); (Lian et al., 2008; Karadzovska et al., 2013). The predicted P values could be used to more easily understand and evaluate the usefulness and safety of topically applied chemical compounds. Thus, similarities between the lipophilicity characteristics or solubility parameters of alternative membranes and human/animal skins may be needed in order to establish a good prediction from various formulations and applied conditions (finite or infinite volume condition).

Strat-M ™ (Merck Millipore, USA) was recently launched and is now commercially available as a skin-mimic artificial membrane. This membrane is

composed of multiple layers of polyester sulfone. However, its potential as an alternative membrane for estimating skin permeation has not yet been clarified.

In the present study, a permeation experiment was performed with Strat-M™, human skin, or hairless rat skin in order to obtain P, DL^{-2}, and KL of the applied compounds from aqueous solution. The usefulness and characteristics of Strat-M™ were investigated by comparing these parameters between human skin, hairless rat skin, and Strat-M ™.

2. Experiment

2.1. Regent and materials

Methyl paraben (MP), ethyl paraben (EP), n-propyl paraben (PP), n-butyl paraben (BP), isosorbide 5-mononitrate (ISMN), n-propyl *p*-aminobenzoate (P-PABA), and n-butyl *p*-aminobenzoate (B-PABA) were purchased from Tokyo Chemical Industry Co., Ltd. (Tokyo, Japan). Lidocaine hydrochloride (LID・HCl) was purchased from Sigma Aldrich (St. Louis, MO, U.S.A.). Antipyrine (ANP), aminopyrine (AMP), methyl *p*-aminobenzoate (M-PABA), and diisopropyl fluorophosphate (DFP) as an ester inhibitor were purchased from Wako Pure Chemical (Osaka, Japan). Ethyl *p*-aminobenzoate (E-PABA) was purchased from Kanto Chemical Co., Ltd. (Tokyo, Japan). Isosorbide dinitrate (ISDN) was kindly gifted from Tokyo Pharmaceutical Industries Industry Co., Ltd. (Tokyo, Japan). The molecular weights (*M.W.*) and octanol/water coefficients (log $K_{o/w}$) of these chemicals are shown in Table 1. Strat-M™ was purchased from Merck Millipore (Billerica, MA, U.S.A.). All other reagents were of HPLC grade and were used without further purification.

Table 1

2.2. Experimental animals

Male hairless rats (WBM/ILA-Ht, 230-280 g) were obtained from the Life Science Research Center, Josai University (Sakado, Saitama, Japan) or Ishikawa Experimental Animal Laboratories (Fukaya, Saitama, Japan). All animal experiments were performed according to the Ethics Committee of Josai University.

2.3. Excised human skin

Excised abdominal human skin (60-year-old Caucasian female) with a thickness of 545 μm was purchased from Biopredic International (Rennes, France) through KAC (Kyoto, Japan). The use of excised human skin was approved by the KAC Ethics Committee for human-derived products.

2.4. Scanning and transmission electron microscopic observations of Strat-M ™

The cross-sectional structure of Strat-M ™ was observed using a scanning electron microscope (SEM) (S-3000N; Jeol Ltd., Tokyo, Japan) operating under a high vacuum condition after being coated with gold. Prior to transmission electron microscopic observations, Strat-M ™ was fixed with 2% osmium tetroxide solution and embedded in epoxy resin. Ultra-thin sections were then prepared with an ultramicrotome. The sections obtained were contrasted with 4% uranyl acetate and observed with a transmission electron microscope (JEM1200-Ex; Jeol Ltd.). The thickness of the skin sections was measured using DP2-BSW software (Olympus Co., Tokyo, Japan).

2.5. Permeation experiments

Strat-M ™: Strat-M ™ was set in a Franz-type diffusion cell (effective diffusion area, 1.77 cm^2) and the receiver chamber was maintained at 32°C. Saturated chemical compounds dissolved in pH7.4 phosphate-buffered saline (PBS), pH 5.0 citrate-buffered saline, or pH 9.0 carbonate-buffered saline (1.0 mL) and 6.0 mL of the corresponding buffer were added to the donor and receiver sides, respectively, in all permeation experiments. The receiver solution was agitated using a stirrer bar and magnetic stirrer throughout the experiments. An aliquot (500 μL) was withdrawn from the receiver chamber and the same volume of fresh buffer was added to the chamber to keep the volume constant. The penetrant concentration in the receiver chamber was determined by HPLC.

Human skin: Frozen human skin was thawed at room temperature and mounted on a Franz-type diffusion cell. In the case of the skin permeation experiments conducted for ester compounds, DFP in PBS at a concentration of 2.7 μmol/mL (6 mL) was added to the receiver chamber for 11 h to prevent metabolism after skin hydration with PBS. The skin permeation experiments were then started. The absence of an effect by DFP on the skin permeation of parabens and other compounds was reported previously (Ahmed et al., 1996; Sugibayashi et al., 2004; Tamura et al., 1995). Permeation experiments were carried out for the other chemical compounds after skin had been hydrated for 12 h with an appropriate buffer at 32°C. A penetrant solution in buffer was added to the donor chamber, whereas DFP in PBS (0.54 μmol/mL) or buffer alone (6 mL each) was added to the receiver chamber to start the permeation experiments. An aliquot (500 μL) was withdrawn from the receiver chamber and the same volume of PBS containing DFP or buffer alone was added to the chamber to keep

the volume constant. Other procedures were followed according to the method described for Strat-M™.

Hairless rat skin: Abdominal skin was cleaned using a wet Kimwipe and excised from hairless rats under anesthesia with an *i.p.* injection of pentobarbital (50 mg/kg). Stripped skin was obtained by stripping the stratum corneum off 20-times with adhesive tape. To decrease variabilities in skin permeability due to the abdominal sites of skin, only skin from the right and left upper abdominal areas were used. Excess fat was trimmed from the excised skin, and the skin sample was set in a Franz-type diffusion cell. The skin permeation experiments were conducted after 60 min of hydration with the corresponding buffer at 32°C. The other procedures were performed with the same experimental method to Strat-M ™.

2.6. Determination of chemicals

The same volume of acetonitrile containing parabens was added to the MP, EP, PP, BP, AMP, ISMN, ISDN, LID, E-PABA, M-PABA, P-PABA, and B-PABA samples. After gentle mixing, the sample was centrifuged for 5 min at 21,500 ×g and 4°C to remove proteins and contaminants. The supernatant was injected onto HPLC. The HPLC system consisted of a pump (LC-10AD; Shimadzu, Kyoto, Japan), Chromatopac (C-R6A; Shimadzu), UV detector (SPD-6A; Shimadzu), system controller (SCL-6B; Shimadzu), and auto-injector (SIL-7A; Shimadzu). The LiChroCART®250-4 column (KGaA·64271; Merck, Darmstadt, Germany) was maintained at 40°C during the eluting mobile phase, 0.1% phosphoric acid : acetonitrile = 75 : 25 for MP and EP, 0.1% phosphoric acid : acetonitrile = 55 : 45 for PP and BP, 0.1% phosphoric acid containing 5 mM sodium dodecyl sulfate : acetonitrile = 50 : 50 for AMP, water : acetonitrile = 55 : 45

for ISDN, 0.1% phosphoric acid containing 5 mM sodium 1-heptanesulfonate : acetonitrile = 70 : 30 for LID, water : acetonitrile = 90 : 10 for ISMN and water : acetonitrile = 80 : 20 for ANP. The flow rate was adjusted to 1.0 mL/min. The injection volume was 20 µL, and detection was performed at 220 nm for ISMN and ISDN, 230 nm for LID, 245 nm for AMP, 254 nm for ANP, and 260 nm for MP, EP, PP and BP. Analyses of E-PABA, M-PABA, P-PABA and B-PABA were carried out with gradient elution systems. A solvent program that initially started with 30% acetonitrile and 70% phosphoric acid solution (0.1%) was changed linearly (13 min) to acetonitrile and phosphoric acid (1 : 1) and held for an additional 10.5 min. The flow rate was maintained at 1.0 mL/min. The system was gradually returned to the starting condition for the next sample. Peaks were detected at 280 nm. The Inertsil® ODS-3 column (4.6 × 150 mm, 5 µm, GL Sciences Inc., Tokyo, Japan) was kept at 40°C.

2.7. Calculation of membrane permeation parameters

Permeation parameters, such as the permeability coefficient and partition and diffusion coefficients, were calculated from the time course of the cumulative amount of chemicals that permeated through membrane by the following equations (Flynn et al., 1974).

$$Flux = \frac{C_v KD}{L} = P \cdot C_v \quad (1)$$

$$DL^{-2} = \frac{1}{6T_{lag}} \quad (2)$$

$$KL = 6T_{lag}P \quad (3)$$

where C_v is the applied concentration of the chemical. The lag time, T_{lag}, was calculated from the x-axis (time-axis) intercept of the slope at a steady-state flux for the permeation profile of chemical compounds through the membrane.

2.8. Statistical analysis

Pearson's correlation coefficient was used to characterize the relationship between log$P$ values in human and rat skins and Strat-M™. Significance was to 5% in all evaluations.

3. Results

Figure 1 shows an SEM image of a vertical section of Strat-M ™. Three layers; i, ii, and iii, were confirmed from the figure. The density of each layer differed and gradually decreased from the top of the membrane. The thicknesses of these layers were 52.3 ± 0.5, 76.7 ± 5.07 and 196 ± 7.37 μm (mean ± S.D.) respectively, from the top, while that of the whole layer was 324.6 ± 4.6 μm.

Figure 1

Figures 2 a, b and c show TEM images of the 1st, 2nd, and 3rd layers of Strat-M™, respectively. Staining was observed in the 1st and 2nd layers, but was absent in the 3rd layer, suggesting that lipids existed in the top two layers.

Figure 2

Figure 3 shows the relationships between log$K_{o/w}$ and log P obtained from permeation experiments through human skin, rat skin, or Strat-M™. Elevations were observed in the log P of all membranes with an increase in lipophilicities of the chemical compounds applied. The relationship obtained between log P and log$K_{o/w}$ could be represented by a sigmoidal curve. The log P values obtained in Strat-M™ were very similar to those in human and rat skins.

Figure 3

Figures 4 a, b, and c show the relationship between log P in human and rat skins, in rat skin and Strat-M™, and in human skin and Strat-M™, respectively and permeability coefficients of chemicals through the membranes were shown in Table 2. A good relationship was observed between the human and rat skin data, as shown in Figure 4a. Furthermore, the almost 1:1 relationship (slope ≈ 1.0) observed between rat and human skin strongly indicated that excised hairless rat could be used as an alternative to human skin. In addition, a good relationship was observed between Strat-M™ and human or rat skin; however, the slopes were slightly greater than unity because the permeation of chemical compounds through Strat-M™ was slightly faster than that through human and hairless rat skins.

Figure 4

Each membrane was characterized using permeation parameters such as

logKL and logDL^{-2}. Figure 5a and b shows the relationship between log$K_{o/w}$ and log KL or logDL^{-2} in Strat-M™, human and rat skins. Log KL in the membranes was increased with an increase of log$K_{o/w}$ of chemicals and these values were almost the same among the membranes, whereas log DL^{-2} in the membranes had almost the constant value despite of different log$K_{o/w}$ of chemicals.

Figure 6a-d shows the relationship for log KL or log DL^{-2} between Strat-M™ and human or rat skin. Log KL in Strat-M™ was similar to that in human or rat skin, and almost 1:1 slopes were observed between Strat-M™ and human or rat skin. On the other hand, logDL^{-2} in Strat-M™ shows liner relationships to those in human or rat skin with higher logDL^{-2} values than those in human and rat skins.

Figure 6

4. Discussion

In vitro permeation experiments using excised human and animal skins are very useful for understanding the skin permeation profiles and skin concentrations of topically applied chemicals. However, *in vitro* experiments using human skin are expensive and sometimes limited due to the low availability of samples and ethical issues. Furthermore, animal testing to evaluate the safety and efficacy of cosmetic ingredients has been banned by Cosmetic Directive 76/768/EEC.

The outmost layer, the stratum corneum, has the largest barrier function against skin permeation by chemicals (Prausnitz and Langer, 2008; Naik et al., 2000; Flynn et al., 1974). In the present study, the rate-limiting step in the permeation of chemicals through Strat-M™ remains unknown because the permeation experiment

could not be performed with each separated layer of Strat-M™. Membrane permeation profiles can generally be expressed by partition and diffusion phenomena (Okamoto et al., 1988). Chemical compounds are immediately distributed or partitioned into the membrane surface following the application of formulations. Thus, the diffusion and partition coefficients of a chemical into a membrane should be investigated to clarify the usefulness of the membrane as an alternative to human skin in permeation experiment.

Elevations were observed in the log P of chemicals through rat and human skins and Strat-M ™ with an increase in their log $K_{o/w}$ (Fig. 3), and 1:1 relationships were detected between human and rat skins or Strat-M ™ (Fig. 4). Furthermore, log KL and log P were similar among membranes at the same log $K_{o/w}$ of chemicals, suggesting that the lipophilicity characteristics or solubility parameters of Strat-M ™ were close to those of human and rat skins. These results suggested that skin permeation by chemicals may be predicted according to their permeability coefficients through Strat-M ™.

To further investigate the characteristics of Strat-M ™, the permeability coefficients of ionized (P_i) and non-ionized (P_u) lidocaines were compared with those through human skin (Kitamura et al., 2009; Hayashi et al., 1992). These values were calculated using skin permeability coefficients at different ratios of the ionized and non-ionized forms of the molecule at pH5.0 and pH7.4 in the present study. P_u and P_i obtained from excised human skin were 7.1×10^{-6} and 4.0×10^{-8} cm/s, respectively. P_u was 177-fold higher than P_i. On the other hand, P_u and P_i obtained from Strat-M™ were 5.6×10^{-6} and 1.3×10^{-7} cm/s, respectively. Although P_u in Strat-M™ was higher than P_i in Strat-M™, P_u in Strat-M™ was only approximately 43-fold higher than P_u in

Strat-M™. P_u in human skin was nearly 1.3-fold higher than that in Strat-M™, whereas P_i in Strat-M™ was nearly 3.2-fold higher than that in human skin. Recent studies have described the main permeation pathway of ionized and large molecular weight compounds. However, the contribution of the hydrophilic pathway such as hair follicles and sweat ducts to total skin permeation by chemical compounds remains unclear. The main permeation route of ionized compounds may be an aqueous-filled pore route due to their high solubility or partition into the aqueous phase. Higher log DL^{-2} in Strat-M™ was observed in hydrophilic chemicals (log $K_{o/w}$<0). Since, diffusivity of chemicals in a membrane is related to its permeation route, low-tortuosity of hydrophilic pathway in Strat-M™ might be a reason for higher permeability of hydrophilic compounds. To confirm this assumption, further *in vitro* permeation experiment was performed with sodium calcein {*M.W.*; 644.5, log $K_{o/w}$; -3.5 (at pH7.4), pK_a; 5.5} and sodium fluorescein {*M.W.*; 376.3, log $K_{o/w}$; -0.61 (at pH7.4), pK_a; 6.4}. These permeations through Strat-M™ were, however, not observed over 8 h experiment, whereas these were observed in human and rat skins (data not shown). The reason for the non-permeation of these chemicals through Strat-M™ might be related to their large molecular sizes. Therefore, physicochemical characteristics of applied chemicals should be considered to use Strat-M™ in a permeation experiment. Further experiment should be performed to reveal the characteristics of aqueous pathway in Strat-M™.

5. Conclusion

The permeability coefficients of chemical compounds through Strat-M™ can be used to predict those through excised human and rat skins, especially for chemical compounds with molecular weights between 151 to 288 and log*Ko/w* from -0.90 to 3.53.

Thus, Strat-M™ can be utilized in screening tests to estimate the permeability of chemicals through human skin. Further experiments need to be conducted with various formulations such as patches, emulsions, and ointments in order to clarify that Strat-M™ can be used to determine formulation designs for the topical and/or transdermal delivery of compounds.

6. Conflict of interest

There is no conflict of interest with any commercial or other associations in this study.

7. Abbreviations

Ko/w; Octanol-water coefficients
P; Permeability coefficient of chemicals
KL; Partition parameter into membrane
DL^{-2}*;* Diffusion parameter in membrane
P_u*;* Permeability coefficient of ionize form of chemicals
P_i*;* Permeability coefficient of non-ionize form of chemicals

6. References

Ahmed, S., Imai, T., Otagiri, M., 1996. Evaluation of Stereoselective Transdermal Transport and Concurrent Cutaneous Hydrolysis of Several Ester Prodrugs of Propranolol: Mechanism of Stereoselective Permeation. Pharm Res 13, 1524–1529.

Akamatsu, M., Fujikawa, M., Nakao, K., Shimizu, R., 2009. In silico prediction of human oral absorption based on QSAR analyses of PAMPA permeability. Chem. Biodivers. 6, 1845–1866.

Avdeef, A., Bendels, S., Di, L., Faller, B., Kansy, M., Sugano, K., Yamauchi, Y., 2007. PAMPA--critical factors for better predictions of absorption. J. Pharm. Sci. 96, 2893–2909.

Bos, J.D., Meinardi, M., 2000. The 500 Dalton rule for the skin penetration of chemical compounds and drugs. Experimental dermatology.

Flynn GL, Yalkowsky SH, Roseman TJ., 1974. Mass transport phenomena and models: theoretical concepts. J. Pharm. Sci.63, 479–510.

Hatanaka, T., Inuma, M., Sugibayashi, K., Morimoto, Y., 1990. Prediction of skin permeability of drugs. I. Comparison with artificial membrane. Chem. Pharm. Bull. 38, 3452–3459.

Hayashi, T., Sugibayashi, K., Morimoto, Y., 1992. Calculation of skin permeability coefficient for ionized and unionized species of indomethacin. Chem. Pharm. Bull. 40, 3090–3093.

Imokawa, G., Abe, A., Jin, K., Higaki, Y., Kawashima, M., Hidano, A., 1991. Decreased level of ceramides in stratum corneum of atopic dermatitis: an etiologic factor in atopic

dry skin? J. Invest. Dermatol. 96, 523–526.

Kano, S., Todo, H., Sugie, K., FUJIMOTO, H., NAKADA, K., Tokudome, Y., Hashimoto, F., Sugibayashi, K., 2010. Utilization of Reconstructed Cultured Human Skin Models as an Alternative Skin for Permeation Studies of Chemical Compounds. Alternatives to animal testing and experimentation : AATEX 15, 61–70.

Karadzovska, D., Brooks, J.D., Monteiro-Riviere, N.A., Riviere, J.E., 2013. Predicting skin permeability from complex vehicles. Advanced Drug Delivery Reviews 65, 265–277.

Keldenich, J., 2009. Measurement and prediction of oral absorption. Chem. Biodivers. 6, 2000–2013.

Kitamura, T., Todo, H., Sugibayashi, K., 2009. Effect of several electrolyzed waters on the skin permeation of lidocaine, benzoic Acid, and isosorbide mononitrate. Drug Dev Ind Pharm 35, 145–153.

Lian, G., Chen, L., Han, L., 2008. An evaluation of mathematical models for predicting skin permeability. J. Pharm. Sci. 97, 584–598.

Morimoto, Y., Hatanaka, T., Sugibayashi, K., Omiya, H., 1992. Prediction of skin permeability of drugs: comparison of human and hairless rat skin. J. Pharm. Pharmacol. 44, 634–639.

Murthy, 2012. Transdermal drug delivery: approaches and significance. RRTD 1-2.

Naik, A., Kalia, Y., Guy, R., 2000. Transdermal drug delivery: overcoming the skin's barrier function. Pharm. Sci. Technol. Today 3, 318–326.

Okamoto, H., Hashida, M., Sezaki, H., 1988. Structure-activity relationship of 1-alkyl- or 1-alkenylazacycloalkanone derivatives as percutaneous penetration enhancers. J. Pharm. Sci. 77, 418-424.

Palac, Z., Engesland, A., Flaten, G.E., Skalko-Basnet, N., 2014. Filipović-Grčić J, Vanić

Z. Liposomes for (trans)dermal drug delivery: the skin-PVPA as a novel in vitro stratum corneum model in formulation development. J Liposome Res. Early Online, 1-10.

Potts, R.O., Guy, R.H., 1992. Predicting skin permeability. Pharm Res 9, 663–669.

Poumay, Y., Dupont, F., Marcoux, S., Leclercq-Smekens, M., H rin, M., Coquette, A., 2004. A simple reconstructed human epidermis: preparation of the culture model and utilization in in vitro studies. Arch Dermatol Res 296, 203–211.

Prausnitz, M.R., Langer, R., 2008. Transdermal drug delivery. Nat Biotechnol 26, 1261–1268.

Riviere, J.E., Brooks, J.D., 2011. Predicting skin permeability from complex chemical mixtures: dependency of quantitative structure permeation relationships on biology of skin model used. Toxicol. Sci. 119, 224–232.

Scott, R.C., Walker, M., Dugard, P.H., 1986. A comparison of the in vitro permeability properties of human and some laboratory animal skins. Int J Cosmet Sci 8, 189–194.

SinkÃ³, B.L., Garrigues, T.M., Balogh, G.T., Nagy, Z.K., Tsinman, O., Avdeef, A., Takács-Novák, K., 2012. European Journal of Pharmaceutical Sciences. Eur J Pharm Sci 45, 698–707.

Sugibayashi, K., Hayashi, T., Matsumoto, K., Hasegawa, T., 2004. Utility of a three-dimensional cultured human skin model as a tool to evaluate the simultaneous diffusion and metabolism of ethyl nicotinate in skin. Drug Metab. Pharmacokinet. 19, 352–362.

Sugibayashi, K., Todo, H., Oshizaka, T., Owada, Y., 2010. Mathematical model to predict skin concentration of drugs: toward utilization of silicone membrane to predict skin concentration of drugs as an animal testing alternative. Pharm Res 27, 134–142.

Tamura, M., Sueishi, T., Sugibayashi, K., Morimoto, Y., Juni, K., Hasegawa, T.,

Kawaguchi, T., 1995. Metabolism of testosterone and its ester derivatives in organotypic coculture of human dermal fibroblasts with differentiated epidermis. Int J Pharm 131, 263–271.

Tehan, B.G., Lloyd, E.J., Wong, M.G., Pitt, W.R., Gancia, E., Manallack, D.T., 2002. Estimation of pKa Using Semiempirical Molecular Orbital Methods. Part 2: Application to Amines, Anilines and Various Nitrogen Containing Heterocyclic Compounds. Quantitative Structure - Activity Relationships. Wiley Online Library 21, 473–485.

Todo, H.H., Kimura, E.E., Yasuno, H.H., Tokudome, Y.Y., Hashimoto, F.F., Ikarashi, Y.Y., Sugibayashi, K.K., 2010. Permeation pathway of macromolecules and nanospheres through skin. Biol Pharm Bull 33, 1394–1399.

Tokudome, Y., Jinno, M., Todo, H., Kon, T., Sugibayashi, K., Hashimoto, F., 2011. Increase in ceramide level after application of various sizes of sphingomyelin liposomes to a cultured human skin model. Skin Pharmacol Physiol 24, 218–223.

Yamashita, S., Tanaka, Y., Endoh, Y., Taki, Y., Sakane, T., Nadai, T., Sezaki, H., 1997. Analysis of drug permeation across Caco-2 monolayer: implication for predicting in vivo drug absorption. Pharm Res 14, 486–491.

Figure captions.

Figure 1　Scanning electron microscopic image of a cross-section of Strat-M™. The first i), second ii), and third layer iii) of Strat-M™.

Figure 2　Transmission scanning electron microscopic observation of a cross-section of Strat-M™.　The first i), second ii), and third layer iii) of Strat-M™.　Lipids in the layer were stained with a black color.　Arrows show the lipid region.

Figure 3 Relationships between log $K_{o/w}$ and log P of applied chemical compounds. Symbols; Excised human skin (△), excised hairless rat skin (○), and Strat-M ™ (□).　All results are expressed as the means ± S.E. (n=3).

Figure 4　Relationships between log P values of human skin and rat skin or Strat-M ™. All results are expressed as the means ± S.E. (n=3). Pearson's Correlation Coefficient showed significance (P <0.05).

Figure 5　Relationships between log $K_{o/w}$ and log KL, *or* log DL^{-2} of applied chemical compounds through human skin and rat skin or Strat-M ™..　Symbols; Excised human skin (△), excised hairless rat skin (○), and Strat-M ™ (□).　All results are expressed as the means ± S.E. (n=3).

Figure 6　Relationships in logKL (a, b) or log D (c, d) between Strat-M™ and human skin or rat skin.　(a, c); Strat-M™ vs human skin, (b,d); Strat-M™ vs human skin.　All

results are expressed as the means ± S.E. (n=3). Pearson's Correlation Coefficient showed significance ($P<0.05$).

Table 1　Physicochemical properties of the compounds used in the present study

	Abbreviation	*M.W.*	log$K_{o/w}$*
			-0.9 (pH5.0)
Lidocaine	LID	288.8	1.3 (pH7.9)
			1.4 (pH10)
Isosorbide 5-mononitrate	ISMN	191.1	-0.2 (pH7.4)
Caffeine	CAF	194.2	-0.12 (pH7.4)
Aminopyrine	AMP	231.3	1.1 (pH7.4)
Isosorbide dinitrate	ISDN	236.1	1.2 (pH7.4)
Methyl paraben	MP	152.2	1.9 (pH7.4)
Ethyl paraben	EP	166.1	2.3 (pH7.4)
n-Propyl paraben	PP	180.2	2.8 (pH7.4)
n-Butyl paraben	BP	194.2	3.5 (pH7.4)
Methyl *p*-amimobenzoate	M-PABA	151.6	1.38 (pH7.4)
Ethyl *p*-amimobenzoate	E-PABA	165.2	1.89 (pH7.4)
n-Propyl *p*-amimobenzoate	P-PABA	179.2	2.43 (pH7.4)
n-Butyl *p*-amimobenzoate	B-PABA	193.2	2.70 (pH7.4)

*Octanol/buffer partition coefficient of compounds at 32°C.

pH was adjusted with pH 7.4 phosphate-buffered saline, pH 5.0 citrate-buffered saline, or pH 9.0 carbonate-buffered saline.

Table 2 Permeability coefficients of chemical through Strat-M™, hairless rat skin and human skin

Compounds	P (cm/s) $\times 10^{-6}$ Strat-M™	P (cm/s) $\times 10^{-6}$ Hairless rat skin	P (cm/s) $\times 10^{-6}$ Human skin
MP	4.02 ± 0.60	2.39 ± 0.31	2.49 ± 0.03
EP	4.21 ± 0.20	2.96 ± 0.06	3.86 ± 0.49
PP	4.01 ± 0.16	3.63 ± 0.15	3.63 ± 0.15
BP	4.24 ± 0.34	2.31 ± 0.26	3.54 ± 0.18
ISMN	0.15 ± 0.02	0.07 ± 0.01	0.11 ± 0.01
AMP	0.87 ± 0.25	0.29 ± 0.11	0.33 ± 0.02
ISDN	3.14 ± 0.01	2.57 ± 0.15	3.14 ± 0.17
LCH (pH5.0)	0.14 ± 0.02	0.04 ± 0.01	0.05 ± 0.02
LCH (pH10)	5.55 ± 0.53	9.21 ± 3.68	1.97 ± 0.15
LCH (pH7.9)	1.20 ± 0.12	1.30 ± 0.11	0.14 ± 0.01
CAF	0.47 ± 0.07	0.26 ± 0.02	0.18 ± 0.02
M-PABA	8.95 ± 0.26	7.22 ± 0.17	18.4 ± 0.83
E-PABA	11.25 ± 0.41	10. 6 ± 0.25	20.1 ± 2.24
P-PABA	13.55 ± 0.58	19.6 ± 1.61	22.3 ± 3.03
B-PABA	10.14 ± 0.53	9.49 ± 0.79	20.1 ± 3.02

Mean ± S.E. (n=3)

Figure 1

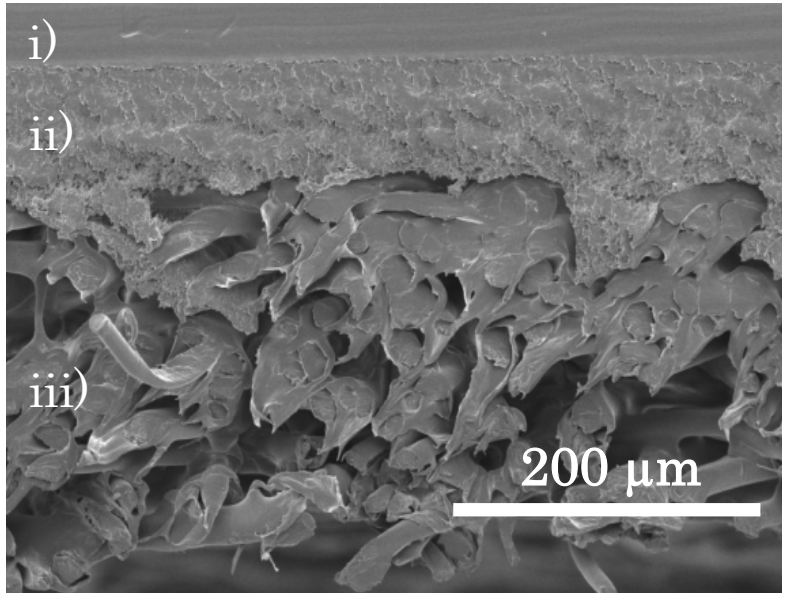

Figure 2

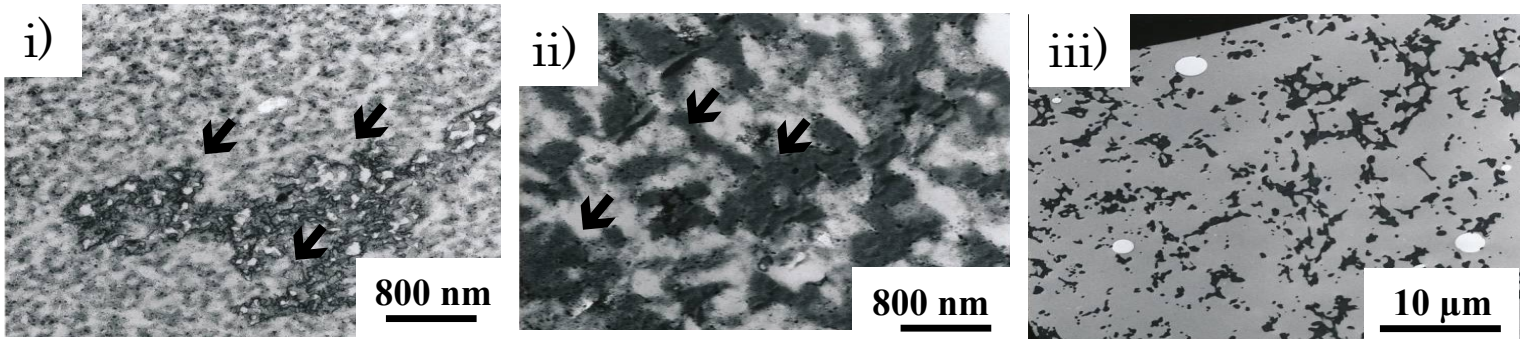

Figure 3

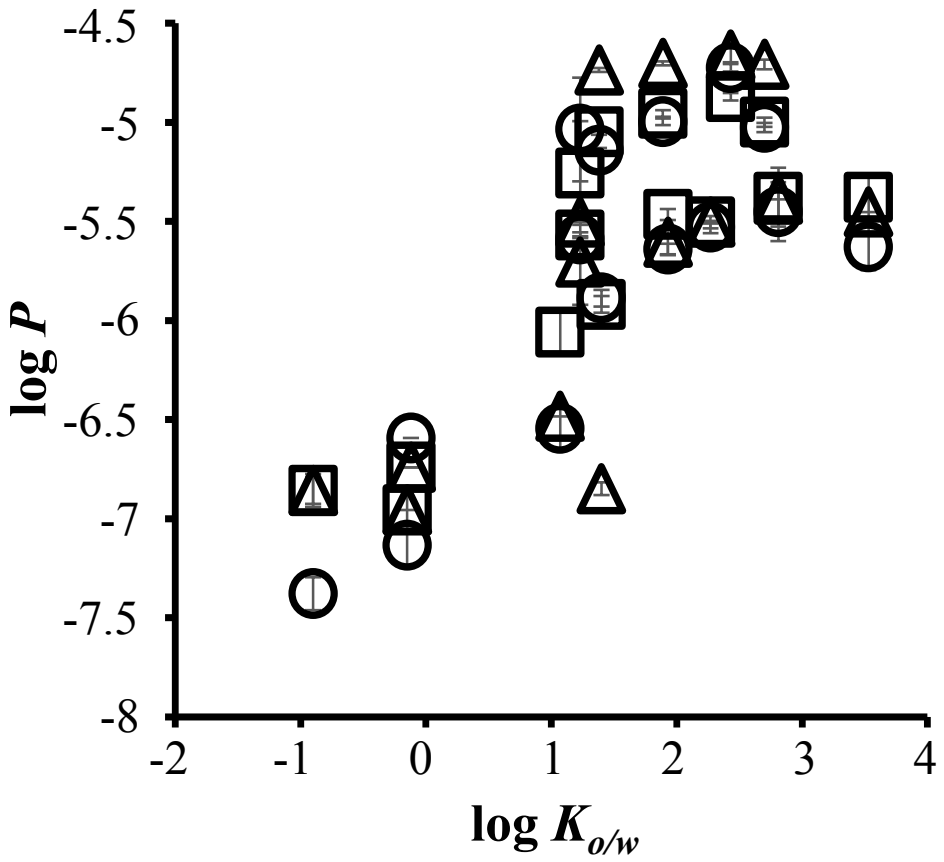

Figure 4

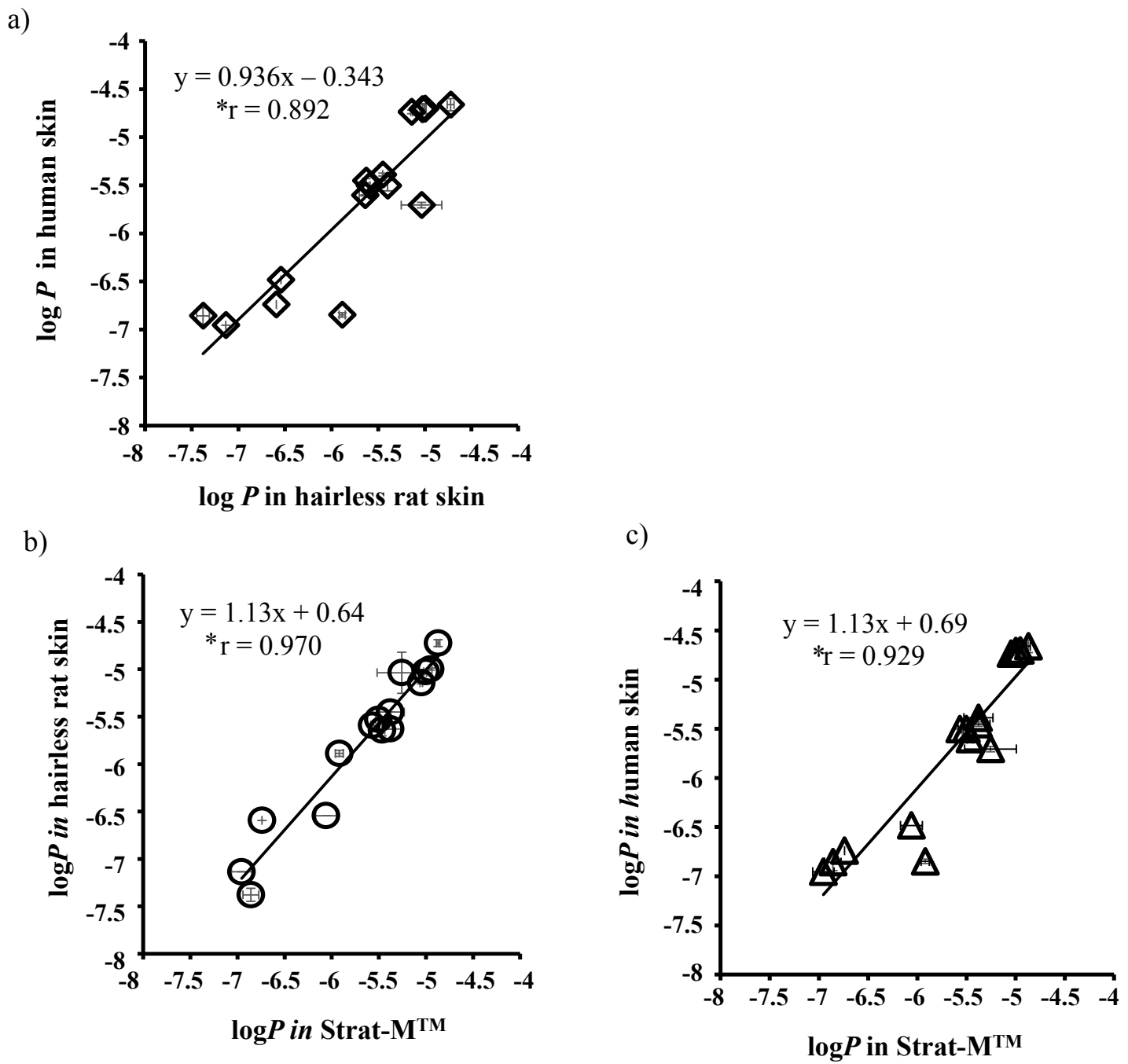
a)
y = 0.936x – 0.343
*r = 0.892
log P in human skin
log P in hairless rat skin
b)
y = 1.13x + 0.64
*r = 0.970
logP in hairless rat skin
logP in Strat-M™
c)
y = 1.13x + 0.69
*r = 0.929
logP in human skin
logP in Strat-M™

Figure 5

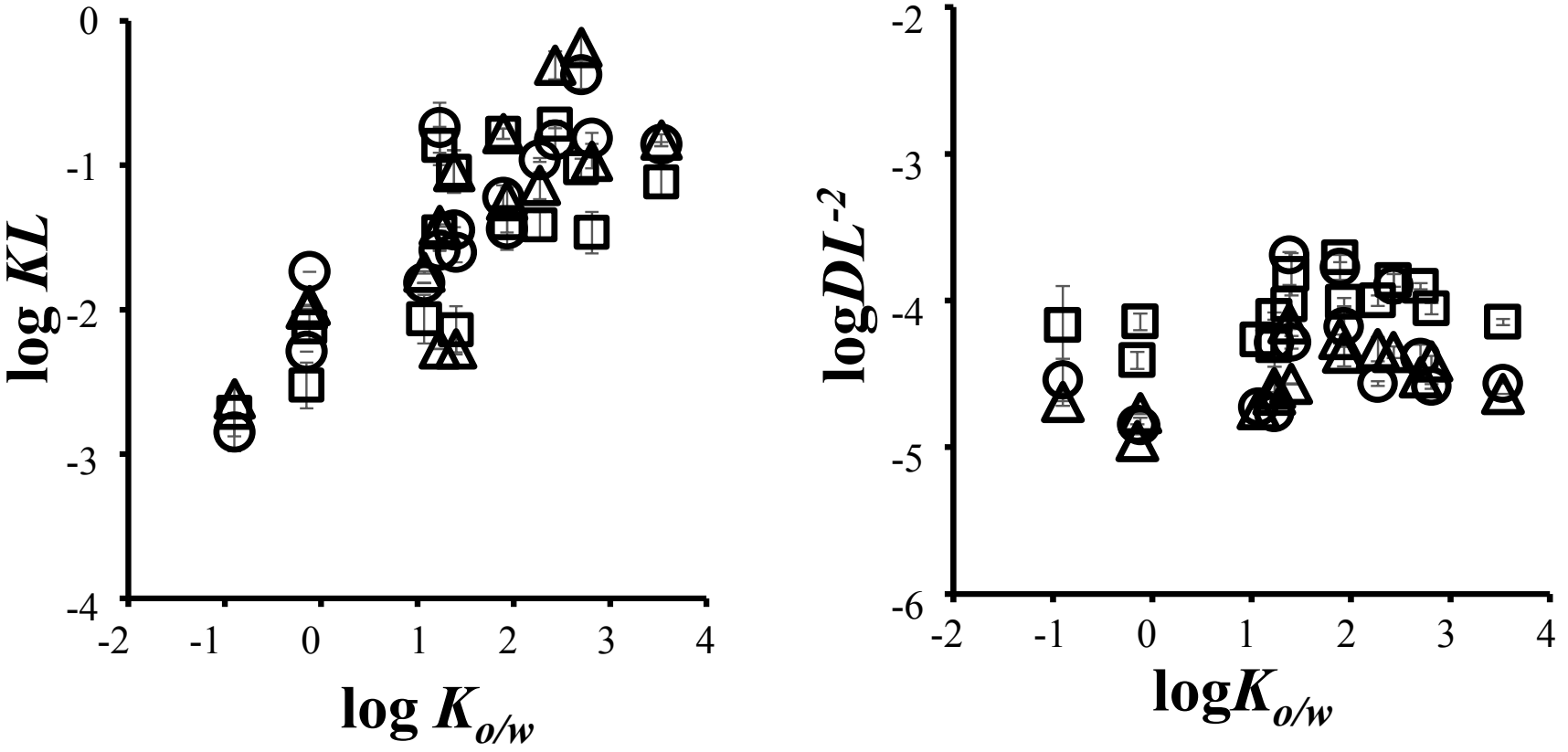

Figure 6

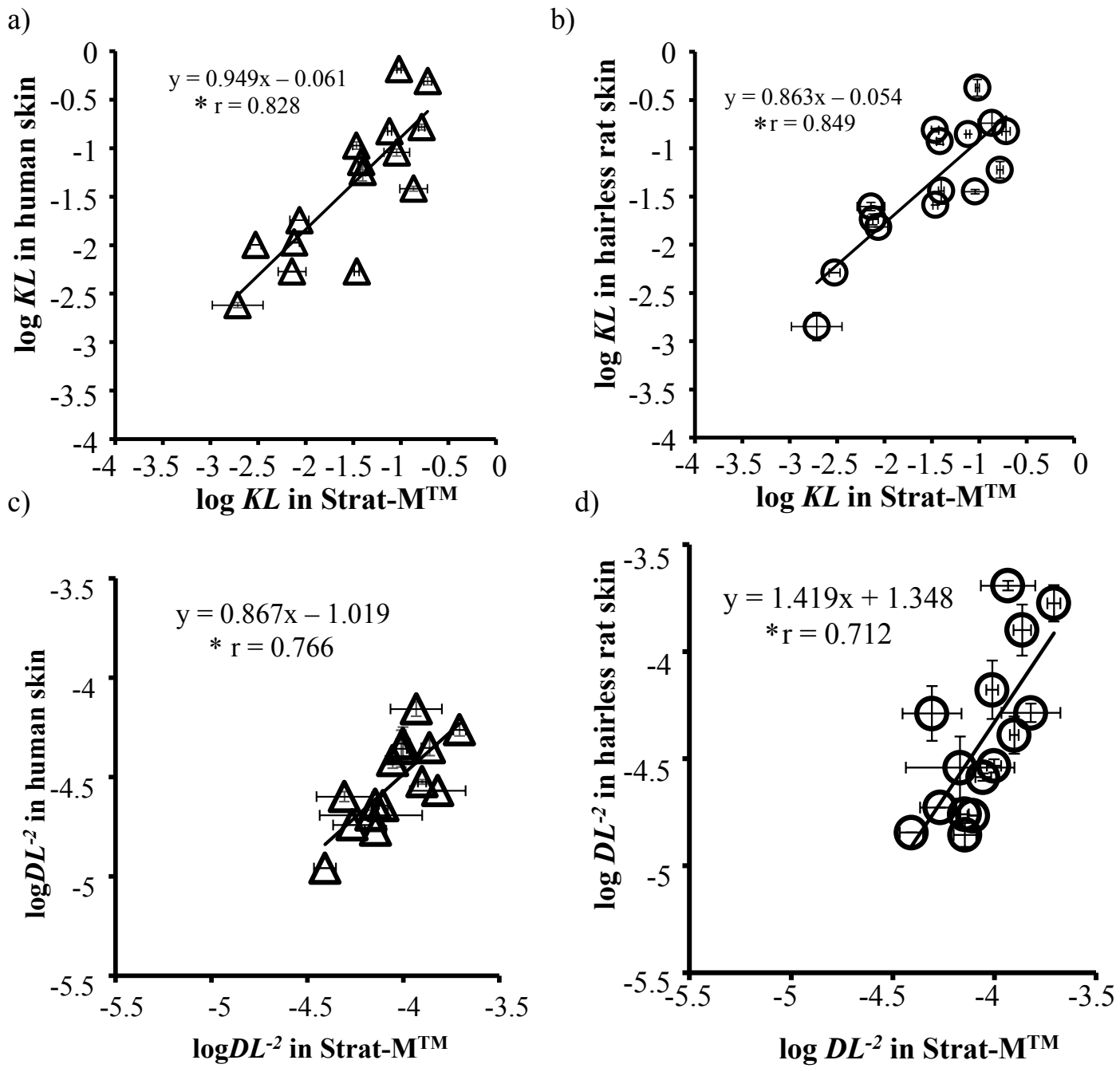
a)
y = 0.949x – 0.061
* r = 0.828
log KL in human skin
log KL in Strat-M™
b)
y = 0.863x – 0.054
*r = 0.849
log KL in hairless rat skin
log KL in Strat-M™
c)
y = 0.867x – 1.019
* r = 0.766
logDL-2 in human skin
logDL-2 in Strat-M™
d)
y = 1.419x + 1.348
*r = 0.712
log DL-2 in hairless rat skin
log DL-2 in Strat-M™